

BR874912

UNIVERSIDADE DE SÃO PAULO

PUBLICAÇÕES

**INSTITUTO DE FÍSICA
CAIXA POSTAL 20516
01498 - SÃO PAULO - SP
BRASIL**

IFUSP/P-569

STATISTICAL DECAY OF GIANT RESONANCES

by

H. Dias, N. Teruya and E. Wolyneć

Instituto de Física, Universidade de São Paulo

Fevereiro/1986

STATISTICAL DECAY OF GIANT RESONANCES

H. DIAS, N. TERUYA AND E. WOLYNEC

INSTITUTO DE FISICA DA UNIVERSIDADE
DE SAO PAULO, SAO PAULO, SP, BRAZIL

1986

ABSTRACT

Statistical calculations to predict the neutron spectrum resulting from the decay of Giant Resonances are discussed. The dependence of the results on the optical potential parametrization and on the level density of the residual nucleus is assessed. A Hauser-Feshbach calculation is performed for the decay of the monopole giant resonance in ^{208}Pb using the experimental levels of ^{207}Pb from a recent compilation. The calculated statistical decay is in excellent agreement with recent experimental data, showing that the decay of this resonance is dominantly statistical, as predicted by continuum RPA calculations.

1. Introduction

Since Giant Resonances (GR's) have mostly excitation energies above particle emission thresholds, they usually decay by particle emission. In a microscopic picture, the excitation of a GR is described as a coherent superposition of 1p-1h excitations of the nucleus. The decay of these 1p-1h configurations can proceed by particle emission, leading to the population of hole states in the residual nucleus (direct decay), or they can mix with more complex 2p-2h configurations. These more complex 2p-2h configurations can in turn decay either by emission of a particle, or they can mix with still more complex 3p-3h configurations. The mixing with more complicated configurations continues until, finally, complete equilibrium has been reached. The resulting compound nuclear state has no memory of the way in which it has been formed, except for the usual conservation of quantum numbers such as spin, parity and excitation energy.

On the basis of the above considerations the observed width of GR's are described as:

$$\Gamma_{\text{tot}} = \Gamma^{\uparrow} + \Gamma^{\downarrow} + \Gamma^{\ast} \quad (1)$$

where Γ^{\uparrow} is the escape width due to the intrinsic width of the 1p-1h states and Γ^{\downarrow} is the spreading width due to coupling of 1p-1h states to more complex states leading to equilibrium.

The values of Γ^+ and Γ^* can be, in principle, determined by studying the decay properties of GR's. Particle decay of $1p-1h$ states will populate, preferentially, specific hole states in the final nucleus, while the decay of the compound state will lead to population of many more levels in the residual nucleus and is governed by transmission coefficients and level densities. In Eq. (1), Γ^* represents the width for preequilibrium emission.

Because the decay properties of GR's are of special interest for understanding the structure and dynamics of these collective modes of nuclear excitations, considerable effort has been concentrated in coincidence experiments where the energy spectrum of the emitted particle is measured. These spectra are compared with the predictions of statistical calculation in order to obtain the relative intensity of statistical to direct and preequilibrium decay. However, these calculations have been performed, in most cases, under very unrealistic assumptions which invalidate the conclusions.

It has been shown recently⁽¹⁾ that if a Hauser-Feshbach calculation^(2,3) is performed using the known levels of ^{207}Pb , instead of a level density function, the measured neutron spectrum, resulting from the decay of the E0 GR, can be completely explained on a statistical basis. In contrast, the assumption that the neutron spectrum, $N(E_n)$, resulting from the decay of the compound state is of the form:

$$N(E_n) \propto E_n \exp(-E_n/T) \quad (2)$$

where E_n is the energy of the emitted neutron and T is a constant nuclear temperature, leads to the conclusion that 15 percent of the decay is non statistical⁽⁴⁾.

In this paper we assess the approximations that lead to Eq. (2) by comparing them with experimental level densities and transmission coefficients. The influence of different parametrizations of the optical potential in the transmission coefficients and their effect in the predicted statistical decay spectrum is also discussed. The predicted statistical decay of the EO GR in ^{208}Pb is recalculated using 63 additional levels from a recent compilation⁽⁵⁾ and compared with the previous calculation⁽¹⁾ and with more complete recent experimental data⁽⁶⁾ for the decay of this resonance.

2. Statistical Decay

The Hauser-Feshbach formalism^(2,3) assumes that the nucleus is excited at an energy E_x by some process. The energy E_x is then thermalized and subsequently dissipated through particle emission. The partial cross sections, σ_i , for the various decay channels are governed by penetrabilities. When the only relevant decay channel is the emission of one neutron, the partial cross sections are:

$$\sigma_1(E_x, U_1) = \frac{\sigma_f(E_x) \sum_{s, \ell} T_{s, \ell}^1(E_{n_1})}{\sum_k \sum_{s', \ell'} T_{s', \ell'}^k(E_{n_k})} \quad (3)$$

where $\sigma_f(E_x)$ is the formation cross section that excites the nucleus to the energy E_x ; $T_{s, \ell}^1(E_{n_1})$ is the transmission coefficient for the i th decay, emitting a neutron of energy E_{n_1} and leaving the residual nucleus at the excitation energy U_1 ; $E_{n_1} = E_x - E_t - U_1$; E_t is the threshold energy for neutron emission; s and ℓ are the spin and angular momentum of the ejected particle; and k is the number of accessible levels in the residual nucleus. The various energies involved in the process are schematically shown in Fig. 1. If the nucleus can decay by various particle channels (α , p , n , $2n$...) the only change in Eq. (3) is that the sum over k , in the denominator, goes over all accessible levels in each of the residual nuclei than can be formed.

Most of the experimental data on neutron spectra resulting from the decay of GR's has been compared with Eq. (2) in order to obtain the statistical component of the process. (As an example of recent work see refs. 7 and 8). Thus it is important to review the assumptions that allow to obtain Eq. (2) from Eq. (3). These assumptions are:

- a) The levels of the residual nucleus can be well represented by a continuous level density, $\rho(U)$, independent of spin and parity. This level density is given by:

$$\rho(U) = \rho_0 \exp(U/T) \quad (4)$$

b) The transmission coefficients in Eq. (3) are independent of s and l and directly proportional to E_n , that is,

$$T_{s,l} = \text{cte} \times E_n \quad (5)$$

With these assumptions it is straightforward to obtain (2) from (3). However, it has been shown⁽¹⁾ that the level density given by Eq. (4) has no similarity with the number of experimental levels per energy interval in ^{207}Pb .

The linearity of the transmission coefficients and their independence of l and s is also a very crude approximation. In Figs. 2 to 7 transmission coefficients for $l = 0$ to 5 are shown, calculated with different parametrizations of the optical potential. The straight line in each figure illustrates the effect of assuming a linear transmission coefficient independent of l .

It is clear from the above discussions that Eq. (2) cannot be used to interpret neutron spectra from the decay of GR's, since the maximum excitation energy in the residual nucleus is usually ≤ 8 MeV. For higher excitation energies, evaporation of another neutron will occur and again the residual nucleus will be at an excitation energy ≤ 8 MeV.

In ref. (1) the decay of the EO GR in ^{208}Pb was evaluated using the experimental levels of ^{207}Pb . However,

a recent compilation⁽⁵⁾ shows 141 levels in the range 0-6.1 MeV, while that calculation used only 78 experimental levels. Another criticism that could be made to the results of ref. 1 is the fact that the transmission coefficients were evaluated using a global optical model potential based on experimental data of neutron elastic scattering in the energy range 7-26 MeV⁽⁹⁾. Since the calculation of the decay deals with neutron energies smaller than 7 MeV, such optical potential could be inappropriate. The transmission coefficients obtained with this global optical potential are shown in Figs. 2 to 7 by the dotted curves. All the transmission coefficients were evaluated using the optical model code SCAT2⁽¹⁰⁾.

A recent measurement of differential elastic and inelastic neutron scattering cross sections for ^{208}Pb and ^{209}Bi in the range 4-7 MeV⁽¹¹⁾ certainly provides the best parametrization of the optical potential for neutrons in the range of excitation energies under consideration. The transmission coefficients obtained with this parametrization are shown by the continuous curves in Figs. 2 to 7. In the same figures transmission coefficients resulting from two other parametrizations are shown. The dashed curves show the transmission coefficients obtained using optical model parameters for lead isotopes⁽¹²⁾, based on fitting of experimental data, which yield good agreement between calculated and measured cross sections at 4.7 and 14.6 MeV. Finally, the

dotted-dashed curves show the transmission coefficients obtained using theoretical optical potential parameters, valid for the energy range 1-15 MeV in medium and heavy nuclei⁽¹³⁾. The letter in most cases overestimates the transmission coefficients as compared to the other three parametrizations, which result from fitting of experimental data. It is worthwhile to note that the transmission coefficients decrease rapidly for neutron energies < 2 MeV.

3. Decay of the E0 Giant Resonance in ^{208}Pb .

The influence of the transmission coefficients in the calculated decay will be illustrated computing the decay of the E0 GR in ^{208}Pb . The calculation assumes that the excitation energy in ^{208}Pb is 13.5 MeV. In order to evaluate the decay using Eq. (3) the experimental levels⁽⁵⁾ were used. From the 158 experimental levels in the range 0-6.6 MeV, 73 levels have no assigned spins and parities. For these levels, spins and parities were assigned comparing the experimental distribution of spins and parities with the distribution predicted by the unperturbed particle vibrator model as discussed in ref. (1). The calculation was performed by coupling the single holes (\uparrow) states $3p_{1/2}$ ($\epsilon_{1/2} = 0.0$ MeV), $2f_{5/2}$ ($\epsilon_{5/2} = 0.57$ MeV), $3p_{3/2}$ ($\epsilon_{3/2} = 0.89$ MeV), $1i_{13/2}$ ($\epsilon_{13/2} = 1.63$ MeV), $2f_{7/2}$ ($\epsilon_{7/2} = 2.34$ MeV) and $1h_{9/2}$ ($\epsilon_{9/2} = 3.42$ MeV) to the

states (\vec{R}) 0^+ ($\epsilon_{0+} = 0.0$ MeV), 3^- ($\epsilon_{3-} = 2.6$ MeV), 5^- ($\epsilon_{5-} = 3.19$ MeV), 2^+ ($\epsilon_{2+} = 4.08$ MeV), 4^+ ($\epsilon_{4+} = 4.32$ MeV) and 8^+ ($\epsilon_{8+} = 4.61$ MeV) of ^{208}Pb . The energies (ϵ_j) of the single holes states and the vibrator energies (ϵ_R) used were taken from the experimental results of ^{207}Pb and ^{208}Pb respectively. The theoretical distribution of spins, parities and energies of the states in ^{207}Pb are obtained from the condition:

$$\vec{I} = \vec{R} + \vec{j} \quad \text{with} \quad \epsilon_I = \epsilon_j + \epsilon_R < 6.6 \text{ MeV}$$

In table I the distribution of levels obtained is compared with the experimental levels⁽⁵⁾ in ^{207}Pb . As shown in Table I the agreement between the number of levels per energy interval predicted by our calculation is in excellent agreement with the experimental distribution, as well as the distribution of spins $< 7/2$. The distribution of spins $> 9/2$ in the interval 4-6.6 MeV predicted by our calculation is also in agreement with experiment if we assume that the experimental levels with unknown spins have $I = 9/2$.

Based on the agreement of the present calculation with the measured levels we are led to assume that the experimental levels with unknown spins have $I > 9/2$. Thus the decay spectra were evaluated using the energies, spins and parities of the experimental levels. For those experimental energy levels without spin assignment we assumed $I = 9/2$, that is, the lowest possible I accordingly to our

calculation. (We choose the lowest value because T_ℓ decreases as ℓ increases for a given neutron energy).

In Fig. 8 the predicted decay of an E0 state at $E_x = 13.5$ MeV in ^{208}Pb is shown. The full line is the result obtained with the global optical potential⁽⁹⁾ while the dashed line results from the optical potential parameters determined from recent experimental data for neutron energies in the range 4-7 MeV. The results from both parametrizations are nearly indistinguishable indicating that the global optical potential from J. Rapaport et al⁽⁹⁾ is also adequate. The optical potential parameters from Fu and Perey⁽¹²⁾ also yield a result indistinguishable from the two shown in Fig. 8. The optical potential from Wilmore and Hodgson yield a spectrum similar to the one shown in Fig. 8, but the relative population of low lying states is - 10% smaller. The latter, as already pointed out, does not show good agreement with more recent experimental data for lead.

The effect of including additional levels in ^{207}Pb from a recent compilation is shown in Fig. 9. The full line shows the predicted decay using 141 levels while the dashed line results from the 78 levels used in ref. 1). Both decay spectra were evaluated using the optical potential parameters of ref. 11) and are normalized to the same number of neutrons. An experimental energy resolution of 500 KeV was assumed, representing each neutron line by a gaussian with FWHM equal to the energy resolution. The inclusion of

63 additional levels produces a noticeable change but not as dramatic as could be expected. The reason is that most of the additional levels are at excitation energies higher than 4 MeV in ^{207}Pb and consequently the neutrons emitted to those levels will have energies smaller than 2 MeV. As we have already pointed out the transmission coefficients decrease rapidly for neutrons of less than 2 MeV. (see Figs. 2-7). This is an important point and shows that the excitation energy region where the level density becomes high and could eventually be represented by a continuous level density has its influence decreased because the corresponding transmission coefficients decrease. Thus, the only reliable way to perform a statistical calculation is to use the experimental levels of the residual nucleus and, eventually, a level density for the region of high excitation energy, but not for the whole range of energies accessible in the residual nucleus.

Finally, in Fig. 10 we compare the experimental neutron spectra⁽⁴⁾ with the predicted spectra using the optical parameters of ref. 11) and the 141 experimental levels of ^{207}Pb ⁽⁵⁾. The conclusions from ref. 1) are unchanged. The observed decay can still be explained on a pure statistical basis. However, the normalization between the calculated and measured spectra is arbitrary, since the experimental data does not contain all low energy neutrons and we cannot conclude if the calculated number of

low energy neutrons is in agreement with experiment or not.

In Fig. 11 more recent experimental neutron spectrum from the decay of the E0 GR in ^{208}Pb is shown⁽⁶⁾. The experimental energy resolution is 500 KeV. The spectra, obtained in an (α, α', n) coincidence experiment covers the excitation energy region 12.5 - 15.5 MeV in ^{208}Pb . It is interesting to compare the results of our statistical calculation with this experimental spectrum, since in this case the normalization between calculated and measured spectrum is not arbitrary because the calculation has to be normalized to the total number of neutrons in the experimental spectrum. The full curve in Fig. 11 shows the spectrum predicted by our statistical calculation assuming an excitation energy of 14 MeV, which is the mean experimental excitation energy and is in the peak of the E0 GR accordingly with ref. 6). For this case 158 levels of ^{207}Pb ⁽⁵⁾ were used in the evaluation of Eq. (3) with the optical potential given by ref. 11). The measured spectrum has a maximum excitation energy of ~ 6 MeV while the calculated spectrum goes up to only 6.6 MeV as a consequence of the assumption made for the excitation energy in ^{208}Pb . Due to the wide range of excitation energies covered by the experimental data a more precise calculation should vary the excitation energy, weighting the various excitation energies with the absorption cross section, but there is not enough data to perform it. Instead we can compute the predicted decay spectrum assuming that the energy resolution is the width of the E0 GR, $\Gamma = 2.4 \text{ MeV}$ ⁽⁶⁾,

since the use of a wide range of excitation energy, centered at the peak of the resonance is, in first approximation, equivalent to an energy resolution equal to the width of the resonance. With this approximation we obtain for the neutron decay of the E0 GR in ^{208}Pb the full curve shown in Fig. 12. The agreement with the experimental spectrum is excellent, leading to the conclusion that the decay is dominantly statistical. This result was already predicted by de Haro et al. ⁽¹⁴⁾ performing continuum RPA calculations both in a 1p-1h and 2p-2h basis. The parameters of these calculations were adjusted to reproduce the experimental single particle energies. The 1p-1h gave a width of 100 KeV for the E0 GR corresponding to a direct decay branch of less than 5 percent, which is in agreement with the present analysis, since such small decay branch cannot be excluded. Inclusion of 2p-2h configurations in the calculation leads to a width of about 2.6 MeV, in good agreement with the experimental value of $2.4 \pm 0.3 \text{ MeV}$ ⁽⁶⁾.

Conclusions

Neutron spectra from the decay of giant resonances cannot be compared with the widely used expression:
 $N(E_n) = cte \times E_n \exp(-E_n/T)$, in order to obtain the statistical component of the decay, because the approximations necessary to obtain this expression are too unrealistic.

A Hauser-Feshbach calculation using the experimental levels of the residual nucleus is the correct approach. The results of such calculations are nearly independent of the parametrization of the optical potential, if the latter is based on experimental data. The global optical potential from J. Rapaport et al. ⁽⁹⁾ is adequate. Also the results of these calculations do not depend strongly on the density of states in the upper two MeV of the residual nucleus, because the transmission coefficients drop fast for neutrons of less than ~ 2 MeV.

The comparison of a Hauser-Feshbach calculation, using the experimental levels of ^{207}Pb , with recent experimental data shows that the decay of the E0 GR in ^{208}Pb by neutron emission is dominantly statistical. This result is in agreement with the prediction of continuum RPA calculations.

REFERENCES

1. H. Diaz and E. Wolyneec, Phys. Rev. C30, 1164 (1984).
2. H. Feshbach, Nuclear Spectroscopy, Part B, edited by F. Ajzenberg-Selove (Academic, New York, 1960).
3. E. Vogt, Adv. Nucl. Phys. 1, 261 (1968).
4. W. Eyrich, K. Fuchs, A. Hoffmann, U. Scheib, H. Steur, and H. Rebel, Phys. Rev. C29, 418 (1984).
5. M.R. Schmorak, Nucl. Data Sheets, 43, 383 (1984).
6. S. Brandenburg, Ph.D. Thesis, Rijksuniversiteit Groningen, Netherlands (1985).
7. K. Fuchs, W. Eyrich, A. Hoffmann, B. Mühldorfer, U. Scheib and H. Schösser, Phys. Rev. C32, 418 (1985).
8. K. Okada, H. Ejiri, T. Shibata, Y. Nagai, T. Motobayashi, H. Ohsumi, M. Noumachi, A. Shimizu, and K. Maeda, Phys. Rev. Lett. 48, 1382 (1982).
9. J. Rapaport, V. Kulkarni and R.W. Finlay, Nucl. Phys. A330, 15 (1979).
10. O. Bersillon, SCAT2, Optical Model Code, CEA Bruyeres-le-chotel, France (1979).
11. J.R.M. Annand, R.W. Finlay and F.S. Dietrich, Nucl. Phys. A443, 249 (1985).

12. C.Y. Fu and F.G. Perey, Atomic Nucl. Data Tables 16, 409 (1975).
13. D. Wilmore and P.E. Hodgson, Nucl. Phys. 55, 673 (1964).
14. R. de Haro, S. Krewald and J. Speth, Nucl. Phys. A388, 265 (1982).

FIGURES CAPTIONS

- Fig. 1 - Diagram of the energies involved in Eq. (3) (see text).
- Fig. 2 - Transmission coefficients for $\ell = 0$ and different parametrizations of the optical potential. The straight line represents the assumption of a transmission coefficient independent of ℓ and directly proportional to the neutron energy (see text).
- Fig. 3 - The same as Fig. 2 but for $\ell = 1$.
- Fig. 4 - The same as Fig. 2 but for $\ell = 2$.
- Fig. 5 - The same as Fig. 2 but for $\ell = 3$.
- Fig. 6 - The same as Fig. 2 but for $\ell = 4$.
- Fig. 7 - The same as Fig. 2 but for $\ell = 5$.
- Fig. 8 - Calculated statistical neutron decay spectra for the E0 GR in ^{208}Pb assuming a resolution of 500 KeV. The continuous (dashed) line shows the result obtained with the optical potential of ref. 9) (ref. 11)). The 141 experimental levels of ^{207}Pb that can be reached by the neutron decay are used (see text).
- Fig. 9 - Calculated statistical neutron decay spectra for the E0 GR in ^{208}Pb , using the optical potential of

ref. 11). The dashed line shows the result obtained using 78 experimental levels of ^{207}Pb as in the calculation of ref. 1) and the full line the result obtained using 63 additional levels from a recent compilation. Both spectra are normalized to the same number of neutrons.

Fig. 10 - The curve is the same calculation shown by the full line Fig. 9. The histogram is the experimental neutron spectrum from ref. 4). The calculated spectrum was normalized to fit the intensity of fast neutrons in the experimental spectrum.

Fig. 11 - Calculated neutron spectrum for an excitation energy of 14 MeV in ^{208}Pb and an energy resolution of 500 KeV. The experimental points are from ref. 6). The calculated spectrum is normalized to the total number of neutrons in the experimental spectrum.

Fig. 12 - The same experimental data as in Fig. 11 and the same statistical calculation but for an energy resolution of 2.4 MeV.

TABLE I - Number of experimental levels (Exp) compared with the number of calculated levels (T).

Energy Interval (MeV)	Number of Levels		Number of Levels with $I < 7/2$			Number of Levels with $I > 9/2$			Number of Experimental Levels without Spin Assignment
	Exp	T	Exp	T	T-Exp	Exp	T	T-Exp	
0-1	3	3	3	3	0	0	0	0	0
1-2	1	1	0	0	0	1	1	0	0
2-3	5	3	4	3	-1	1	0	-1	0
3-4	22	19	4	9	5	11	10	-1	7
4-5	47	50	20	23	3	11	27	16	16
5-6,6	80	80	25	24	-1	5	56	51	50
TOTAL	158	156	56	62	6	29	94	73	73

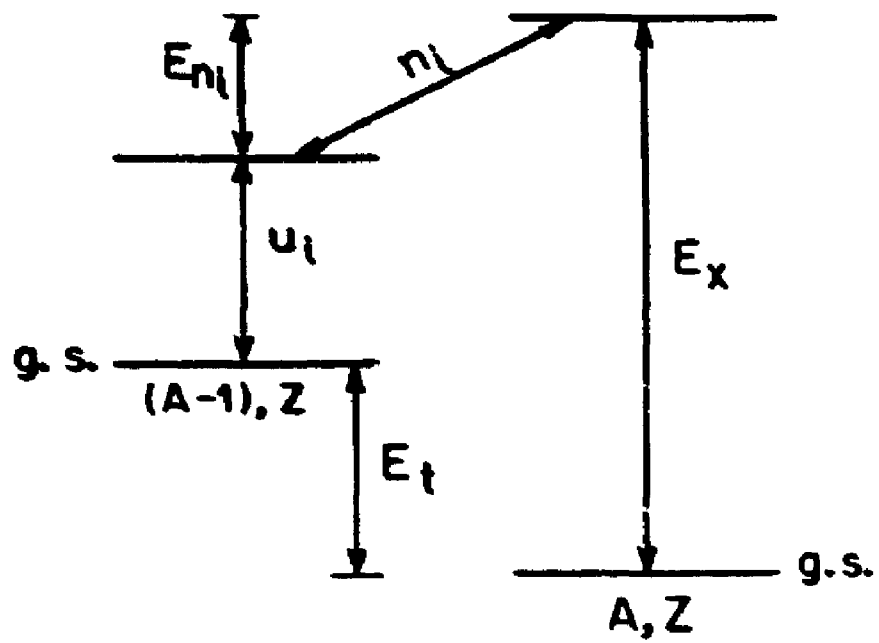


Fig 1

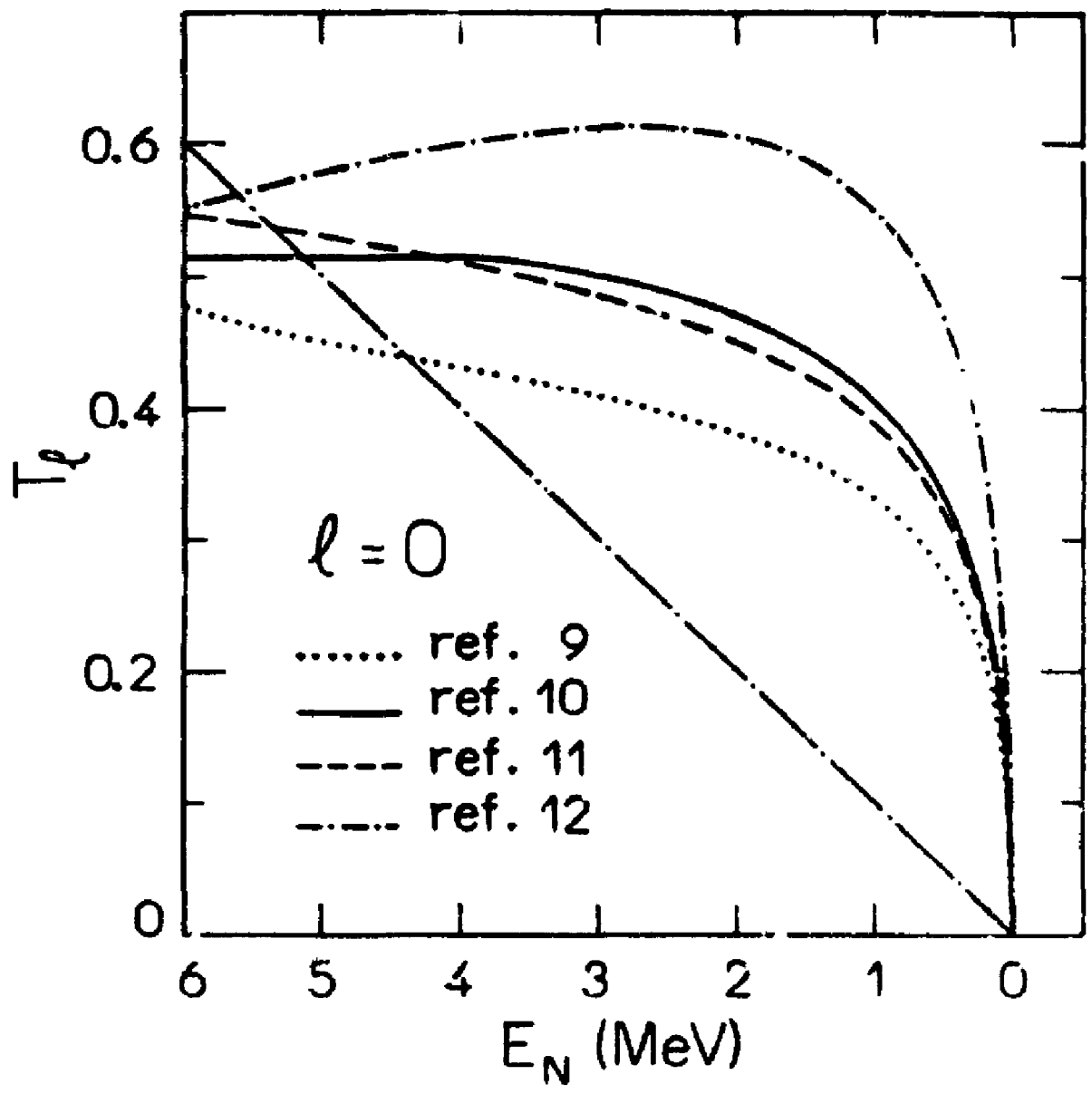


Fig. 2

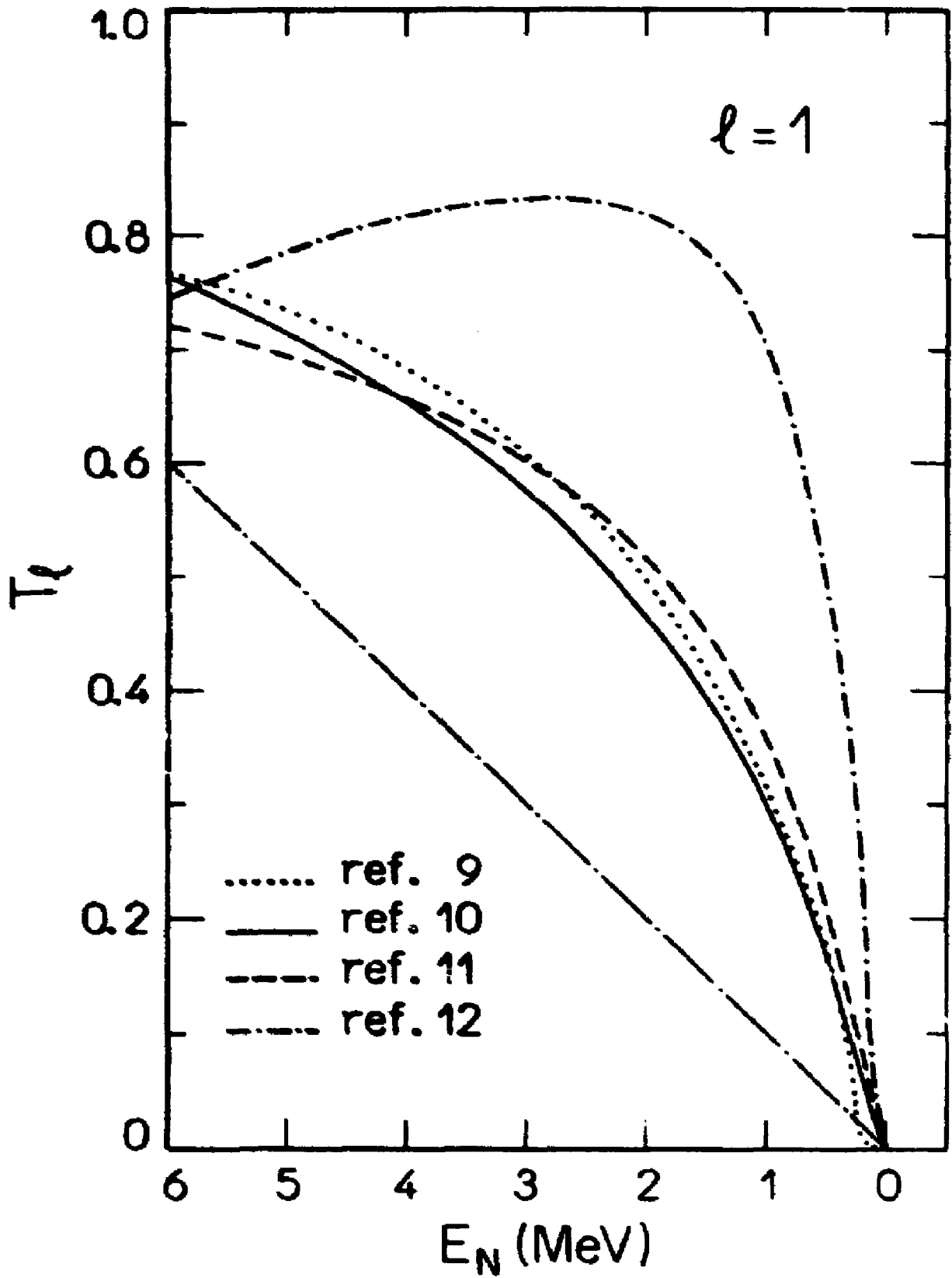


Fig 3

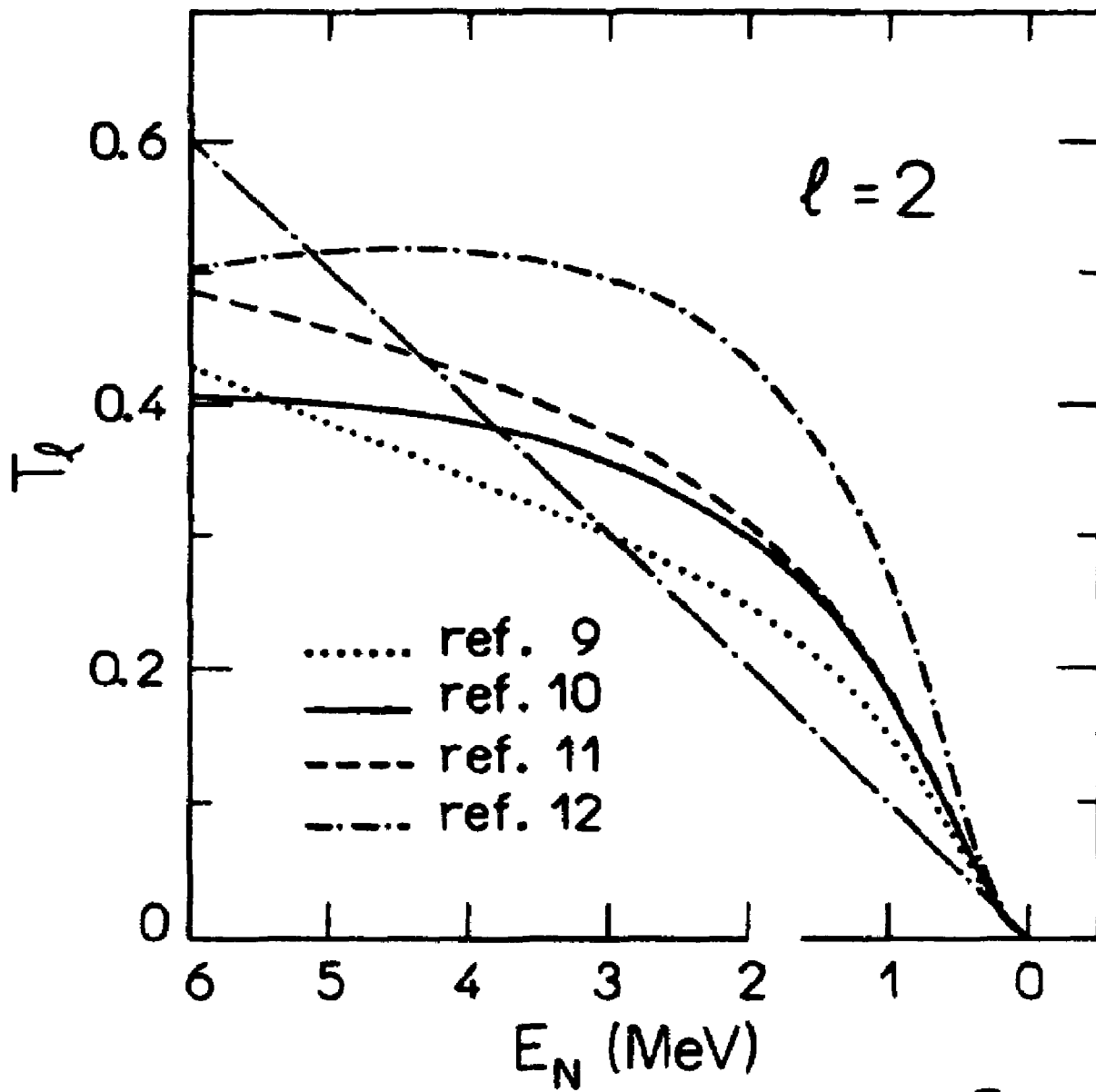


Fig. 4

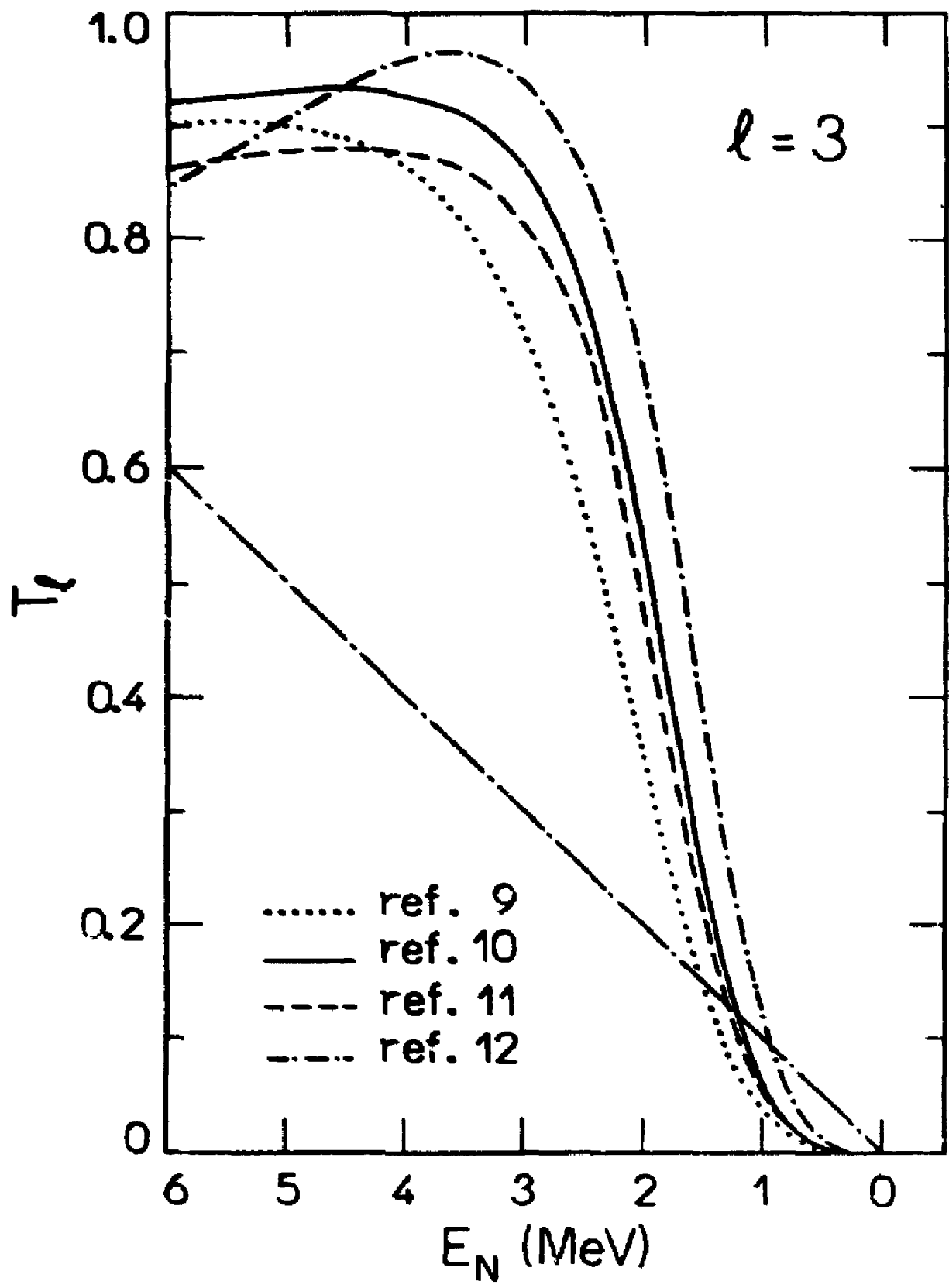


Fig 5

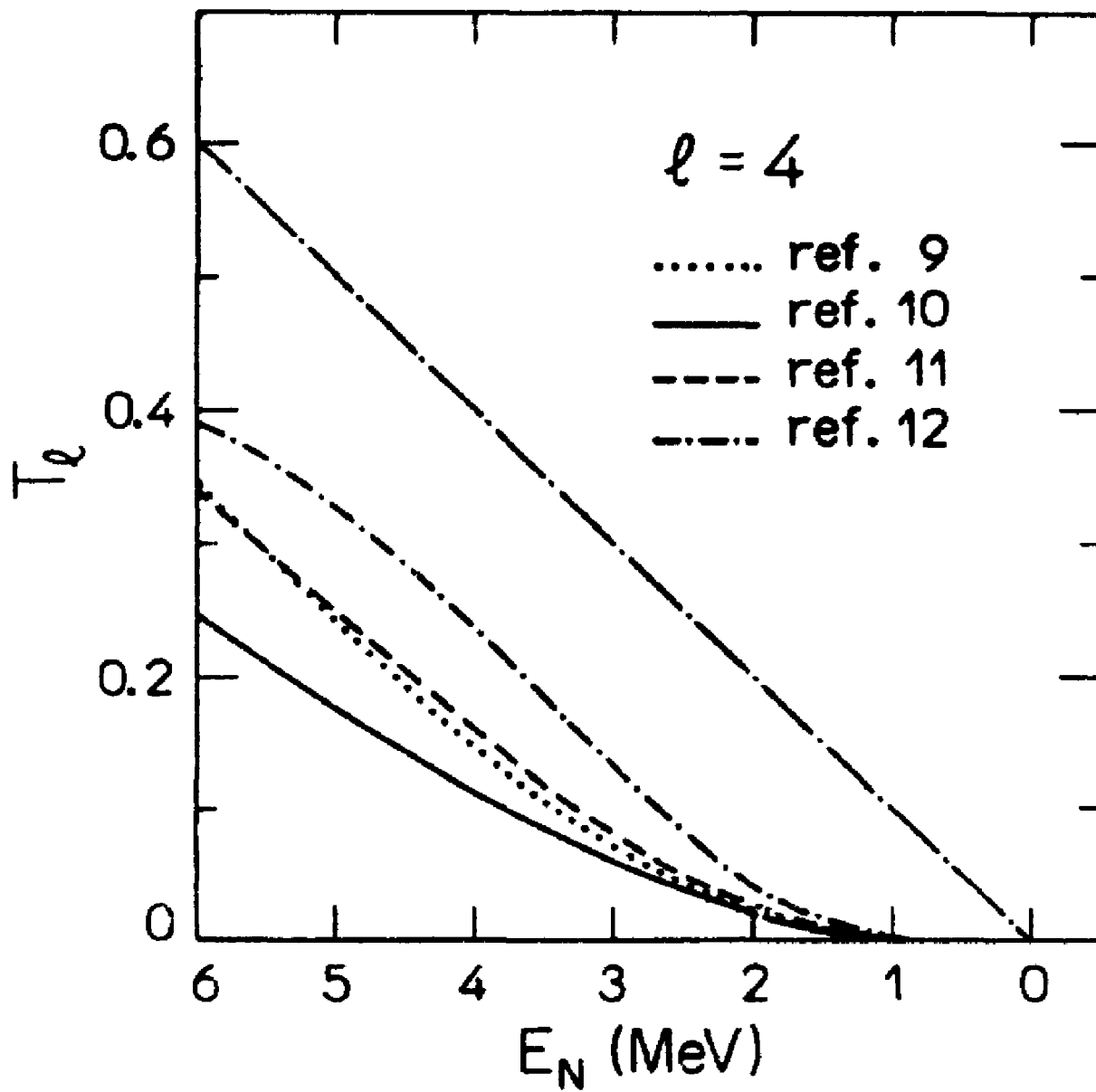


Fig 6

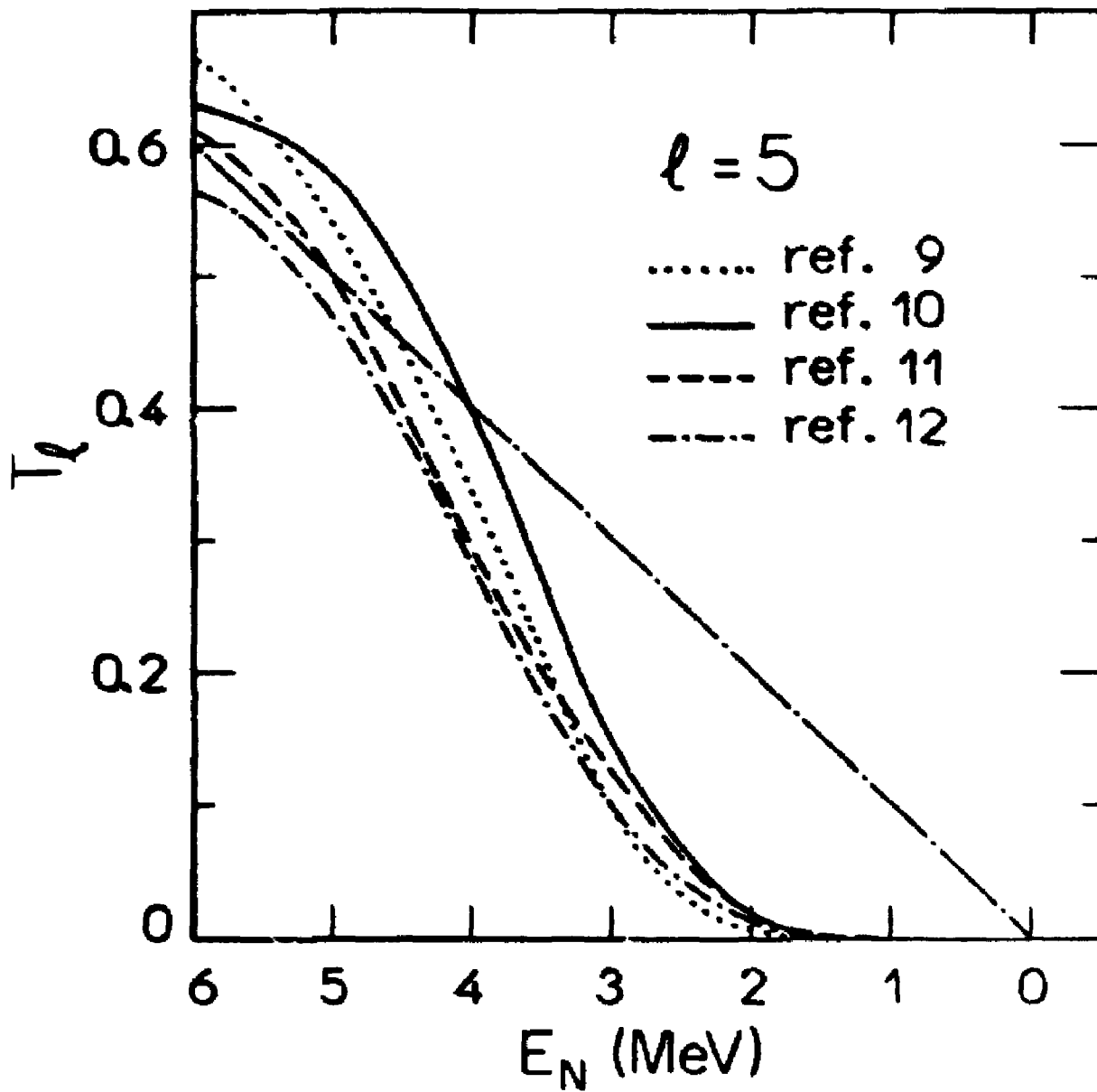


Fig 7

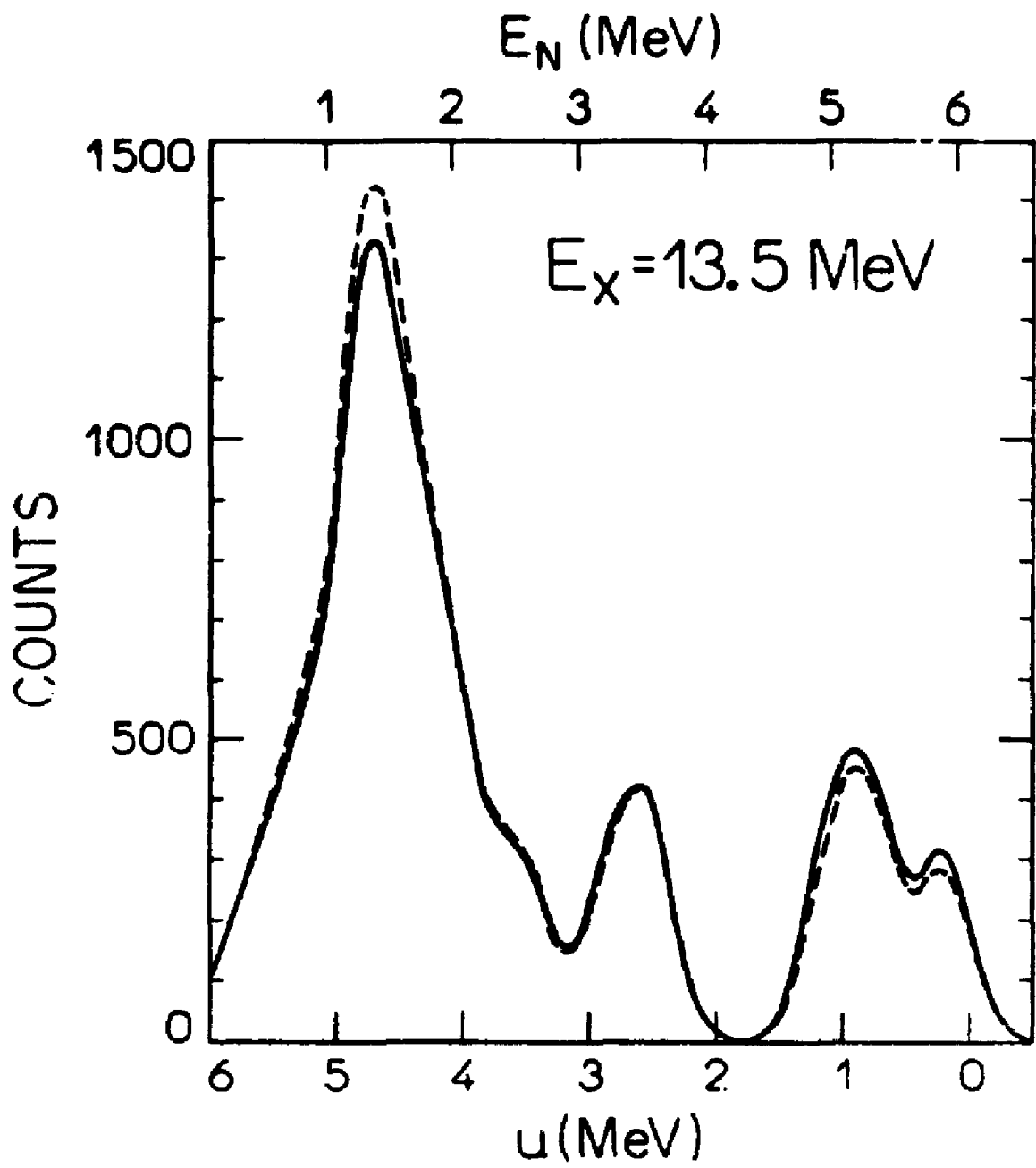


Fig 8

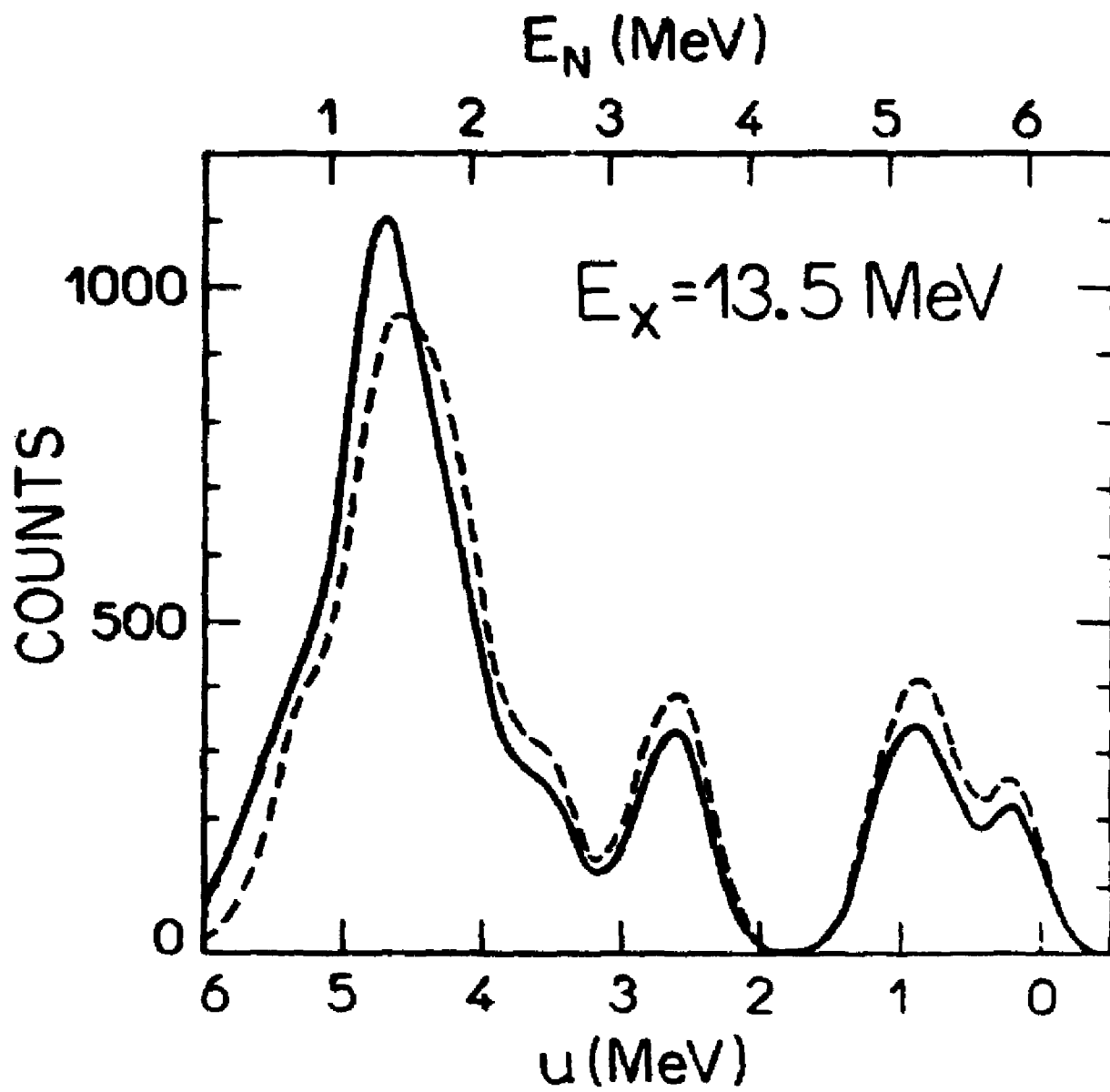


Fig 9

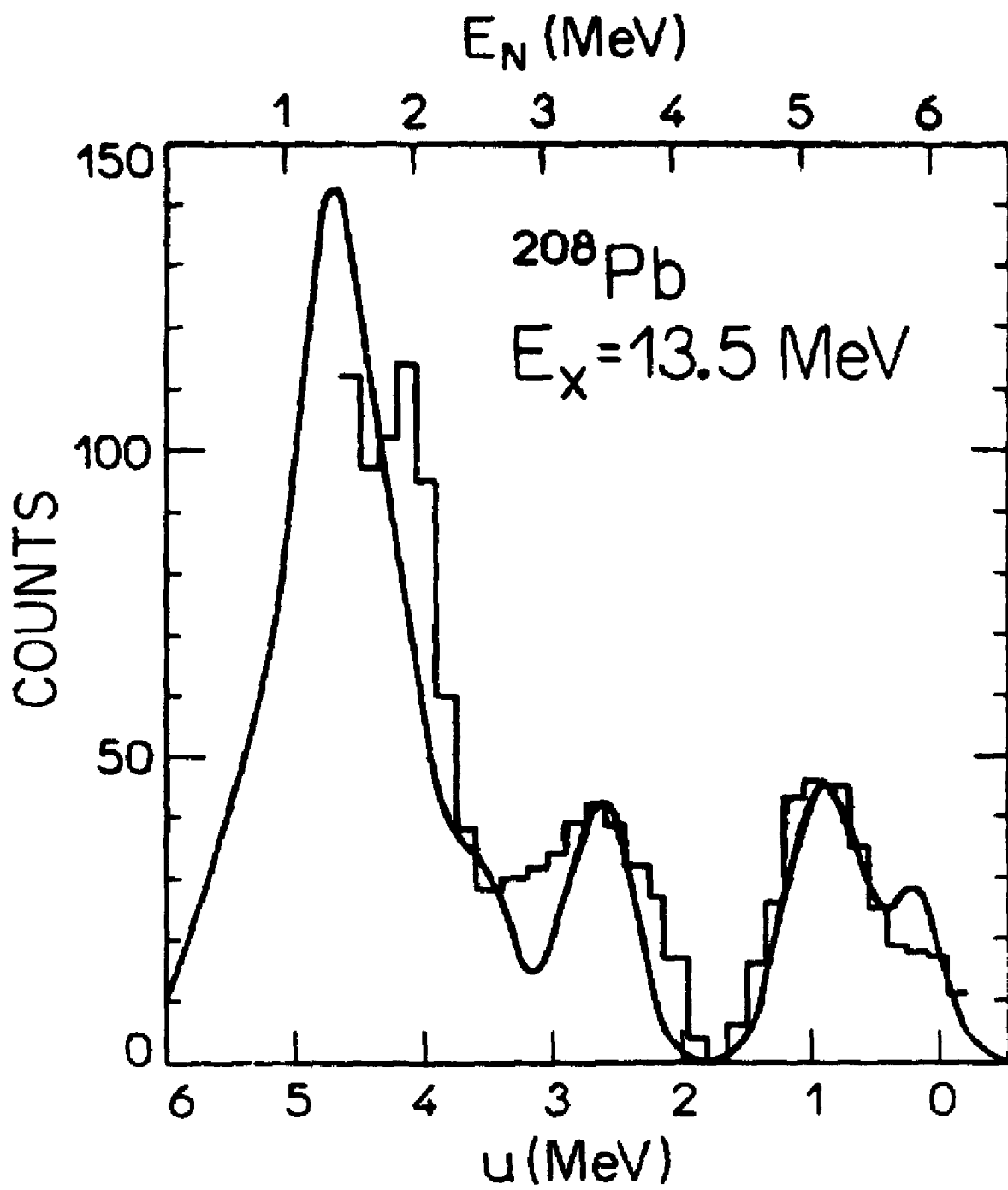


Fig. 10

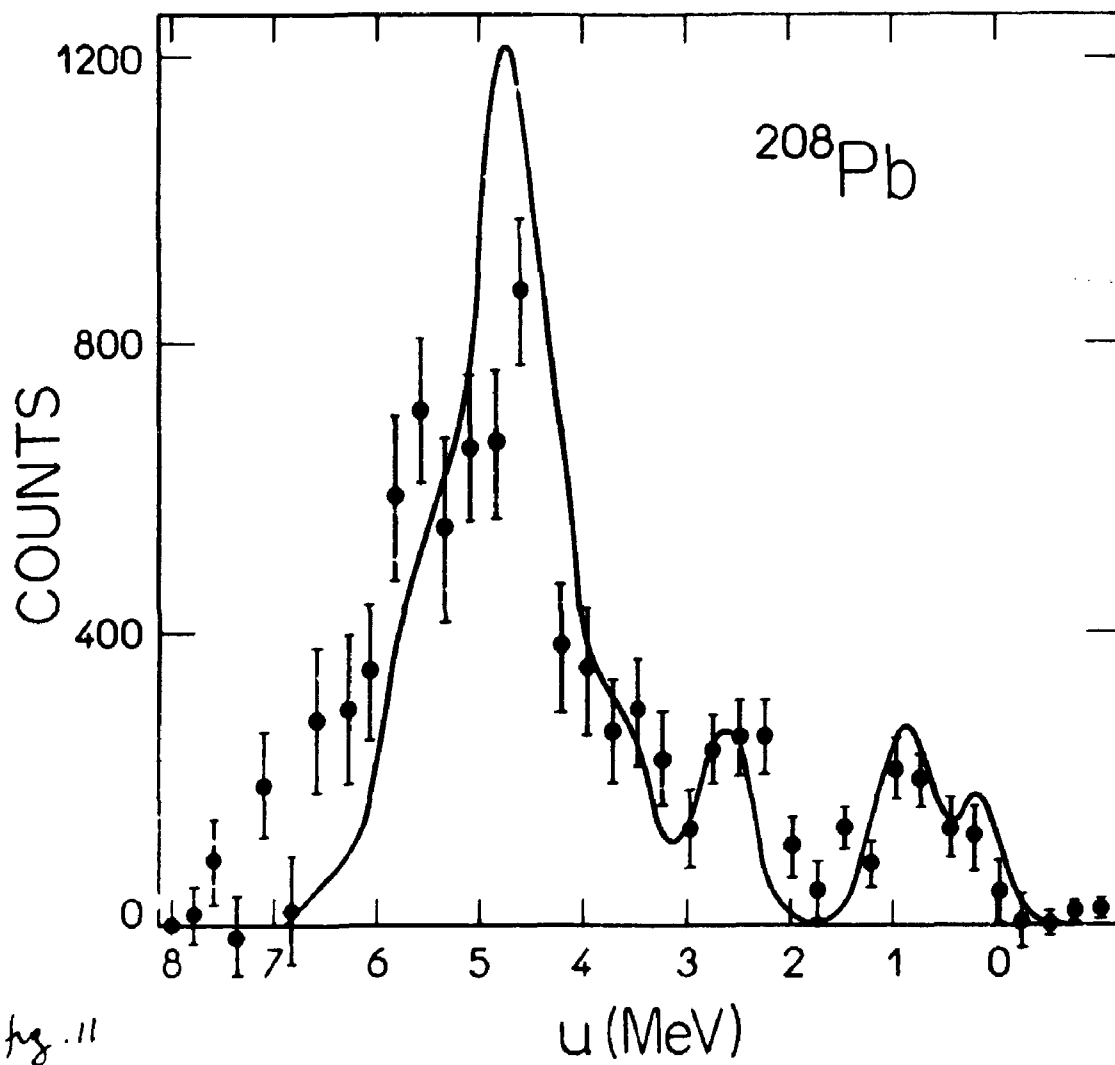


fig. 11

